$^{14}C(\alpha,\gamma)$ reaction rate

E. D. Johnson,* G. V. Rogachev,† J. Mitchell, L. Miller, and K. W. Kemper
Department of Physics, Florida State University, Florida 32306, USA
(Received 14 August 2009; published 22 October 2009)

The $^{14}C(\alpha,\gamma)$ reaction rate at temperatures below 0.3 GK depends on the properties of two near threshold resonances in ^{18}O, the 1^- at 6.198 MeV and the 3^- at 6.404 MeV. The $\alpha + ^{14}C$ asymptotic normalization coefficients for these resonances were determined using the α-transfer reactions $^{14}C(^7Li,t)$ and $^{14}C(^6Li,d)$ at sub-Coulomb energies. The $^{14}C(\alpha,\gamma)$ reaction rate at low temperatures has been evaluated. Implications of the new reaction rate on the evolution of accreting helium white dwarfs and on the nucleosynthesis of low mass stars during the asymptotic giant branch phase are discussed.

DOI: 10.1103/PhysRevC.80.045805 PACS number(s): 21.10.Jx, 25.70.Hi, 26.20.−f, 26.30.−k

I. INTRODUCTION

It has been suggested that the $^{14}C(\alpha,\gamma)^{18}O$ reaction plays an important role in several astrophysical environments. Mitalas [1] pointed out that electron capture on ^{14}N can produce ^{14}C in the degenerate helium core of low-mass stars; the α capture on ^{14}C then follows. It was suggested in Ref. [2] that the $^{14}N(e^-,\nu)^{14}C(\alpha,\gamma)^{18}O$ reaction (NCO reaction) may trigger the helium flash in the core of low-mass stars earlier than the 3α reaction. The significance of the NCO reaction for the evolution of low-mass stars was also considered by Spulak [3], who concluded that it is not effective when compared to the 3α reaction. A contradicting result was obtained by Kaminisi and Arai [4], who used the updated (but still very uncertain) $^{14}C(\alpha,\gamma)$ reaction rate and concluded that the NCO reaction is dominant in igniting the helium flash. While the influence of the NCO reaction on the evolution of low-mass stars in the red giant phase is still uncertain, it was firmly established by Nomoto and Sugimoto [5], and later by Hashimoto *et al.* [6], that the NCO reaction may trigger the helium flash in accreting helium white dwarfs at a lower temperature and density than the 3α reaction. However, this conclusion is rather sensitive to the actual value of the $^{14}C(\alpha,\gamma)$ reaction rate at temperatures between 0.03 and 0.1 GK.

The $^{14}C(\alpha,\gamma)$ reaction is also important in the production of ^{19}F in asymptotic giant branch (AGB) stars. Observations by Jorissen *et al.* [7] show enhanced fluorine abundance in the atmosphere of K, M, MS, S, SC, and C asymptotic giant branch stars. This finding indicates that ^{19}F is produced in these stars, and its abundance can be used to constrain the properties of the AGB models. The path for ^{19}F production in an AGB star, as proposed by Jorissen [7], is rather complex, occurring in the He intershell of the AGB star. Neutrons from the *s*-process neutron generator reaction, $^{13}C(\alpha,n)$, can be captured by ^{14}N, enhanced from the previous CNO cycle. This leads to production of ^{14}C and protons through the $^{14}N(n,p)^{14}C$ reaction. Then ^{18}O is produced by the $^{14}C(\alpha,\gamma)$ reaction or, alternatively, by $^{14}N(\alpha,\gamma)^{18}F(\beta)^{18}O$. The presence of protons and ^{18}O isotopes in the He intershell simultaneously allows the $^{18}O(p,\alpha)^{15}N$ reaction to occur and subsequently $^{15}N(\alpha,\gamma)^{19}F$ capture. Competing reactions that reduce the final abundance of ^{19}F are $^{19}F(\alpha,p)$, $^{18}O(\alpha,\gamma)^{22}Ne$, and $^{15}N(p,\alpha)^{12}C$. A detailed investigation of the ^{19}F production in AGB stars has been performed recently by Lugaro *et al.* [8], and it was determined that the major uncertainties in the production of ^{19}F are associated with the uncertainties in the $^{14}C(\alpha,\gamma)^{18}O$ and $^{19}F(\alpha,p)^{22}Ne$ reaction rates. Addressing uncertainties of the $^{14}C(\alpha,\gamma)$ reaction rate at temperatures relevant to helium flashes in the accreting helium white dwarfs and nucleosynthesis in the asymptotic giant branch stars is the main goal of this work.

Direct measurements of the $^{14}C(\alpha,\gamma)$ reaction cross section are only available for energies above 880 keV in c.m. [9]. The relevant temperature range for accreting helium white dwarfs is between 0.03 and 0.1 GK; for ^{19}F nucleosynthesis in AGB stars, it is ∼0.1 GK. The Gamow window for the $^{14}C(\alpha,\gamma)$ reaction at these temperatures corresponds to an energy range between 50 and 250 keV. At these energies, the cross section for the α-capture reaction on ^{14}C is too low to be measured directly and has to be extrapolated from the higher energy data. However, near-threshold resonances in ^{18}O may have a very strong influence on this extrapolation. The level scheme of ^{18}O is shown in Fig. 1. Three states with excitation energies close to the α-decay threshold at 6.227 MeV are known in ^{18}O. These are the 1^- at 6.198 MeV, the 2^- at 6.351 MeV, and the 3^- at 6.404 MeV. The 2^- state at 6.351 MeV is an unnatural parity state and cannot contribute to the $^{14}C(\alpha,\gamma)$ reaction at any significant level. The 1^- subthreshold state at 6.198 MeV can only contribute to the $^{14}C(\alpha,\gamma)$ reaction through its high-energy tail, therefore its contribution is expected to be relevant only at the lowest energy. Finally, the 3^- state at 6.404 MeV is 177 keV above the α-decay threshold—right in the middle of the energy range of interest.

The strength of a resonance is defined by

$$\omega\gamma = \frac{2J_R+1}{(2j_t+1)(2j_p+1)}\frac{\Gamma_\alpha\Gamma_\gamma}{\Gamma}, \quad (1)$$

where Γ, Γ_α, and Γ_γ are the total, partial α, and partial γ widths and J_R, j_t, and j_p are spins of the resonance, the target, and the projectile. At 177 keV, the partial α width is much smaller than the partial γ width ($\Gamma_\alpha \ll \Gamma_\gamma$), therefore

*edj04@fsu.edu
†grogache@fsu.edu

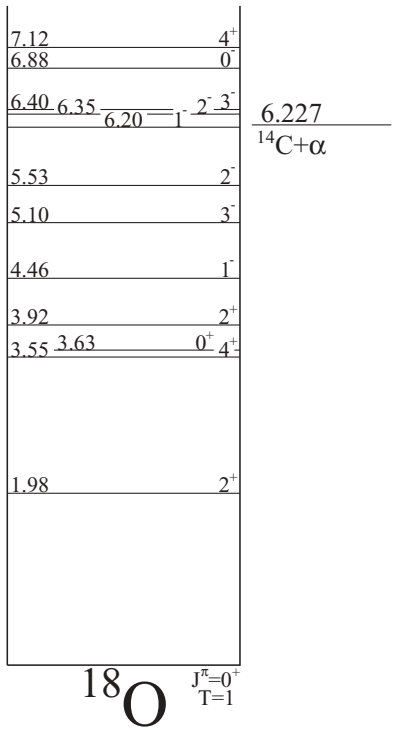

FIG. 1. Partial level scheme of ^{18}O.

the resonant α-capture cross section is determined entirely by the partial α width with resonance strength calculated as $\omega\gamma \approx 7 \times \Gamma_\alpha$ for the 3^- state at 6.404 MeV in ^{18}O. The partial α width of the 3^- state is not known. This leads to several orders of magnitude uncertainty of the ^{14}C(α,γ) reaction rate at $\sim$0.1 GK. The subthreshold 1^- state at 6.198 MeV also contributes to the reaction rate uncertainty at the lowest temperatures.

Information on the partial α widths of resonances in ^{18}O can be extracted using the direct α-transfer reactions ^{14}C(^{6}Li,d) and ^{14}C(^{7}Li,t). Usually these reactions are performed at energies of 5–15 MeV/A and α spectroscopic factors S_α for the states of interest are determined from the distorted-wave Born approximation (DWBA) analysis of the reaction cross sections. The partial α width is then calculated as $\Gamma_\alpha = S_\alpha \times \Gamma_{\rm SP}$, where $\Gamma_{\rm SP}$ is the α single-particle width

$$\Gamma_{\rm SP} = 2P_\ell(kR)\gamma_{\rm sp}^2, \tag{2}$$

$$P_\ell(kR) = \frac{kR}{F_\ell^2(k,R) + G_\ell^2(k,R)}, \tag{3}$$

$$\gamma_{\rm sp}^2 = \hbar^2/\mu R^2, \tag{4}$$

where $P_\ell(kR)$ is a penetrability factor determined by the Coulomb regular and irregular functions $F_\ell(k,R)$ and $G_\ell(k,R)$, μ is a reduced mass, and k is a wave number. R is a channel radius $R = r_0(\sqrt[3]{A_1} + \sqrt[3]{A_2})$, where $r_0 = 1.2$–1.4 fm. The reduced width $\gamma_{\rm sp}$ in Eq. (4) corresponds to the reduced width in a square-well potential. The single-particle width can be calculated more accurately using a realistic Woods-Saxon potential. As is well known, the spectroscopic factor extracted from an α-transfer reaction depends on the parameters of the optical potentials used to describe the wave functions of relative motion in the entrance and exit channels in the DWBA approach and on the shape of the form factor potentials and the number of nodes in the model core-cluster wave function. However, for astrophysical calculations, the asymptotic normalization coefficient (ANC) is needed instead of the spectroscopic factor; and if the transfer reaction is performed at sub-Coulomb energies, then the parametric dependence of the DWBA calculations is greatly reduced. This approach has been applied before in Refs. [10,11], in which the ^{12}C(α,γ) and ^{13}C(α,n) reaction rates due to near-threshold resonances in ^{16}O and ^{17}O were evaluated.

In this work, we measured the cross sections of the ^{14}C(^{7}Li,t) and ^{14}C(^{6}Li,d) α-transfer reactions at sub-Coulomb energies and determined the ANCs of the 1^- and 3^- states in ^{18}O. The discussion is structured as follows: the experimental technique is discussed in Sec. II, the extraction of the ANCs and associated uncertainties are described in Sec. III, the new ^{14}C(α,γ) reaction rate and its astrophysical implications are discussed in Sec. IV, and the conclusions are in Sec. V.

II. EXPERIMENT

The sub-Coulomb α-transfer reactions ^{6}Li(^{14}C,d) and ^{7}Li(^{14}C,t) were performed at the John D. Fox Superconducting Accelerator Laboratory at Florida State University. The use of inverse kinematics, ^{14}C beam and ^{6,7}Li target, has several advantages. First, it eliminates the background associated with (^{6,7}Li,d/t) reactions on the unavoidable ^{12}C admixture to the ^{14}C target. Second, inverse kinematics provides a boost to the light recoils, which is essential for the detection of the reaction products, since the reaction is performed at low sub-Coulomb energies.

Five silicon ΔE-E telescopes were used to detect the light recoils (deuterons/tritons) produced by the α-transfer reaction. The ΔE detectors ranged in thickness from 15 to 25 μm, while the E detectors were 500–1000 μm thick. Particle identification was performed using the standard ΔE-E technique. A sample of the two-dimensional particle identification plot is shown in Fig. 2, where it can be seen that the separation of the different isotopes of hydrogen is sufficient for reliable identification.

The lithium targets were prepared and transferred to the scattering chamber in a sealed container under vacuum to prevent oxidation. The thickness of the lithium targets was $\approx$20 μg/cm^2, and they were prepared on a Formvar backing. An accurate determination of the target thicknesses and detector solid angles was performed using elastic scattering of protons. The $p + ^{6,7}$Li elastic scattering cross section at 95° with proton beam energy of 6.868 MeV was measured previously with a 3% accuracy in Ref. [12], and this result allowed the product of the target thickness and the telescope solid angles to be determined by placing the telescopes at 95° with respect to the beam axis one by one and measuring $p + ^{6,7}$Li elastic scattering with each lithium target.

For energies below the Coulomb barrier, the angular distribution for a direct transfer reaction has a peak at back angles, 180° in the c.m. frame, which corresponds to a peak at

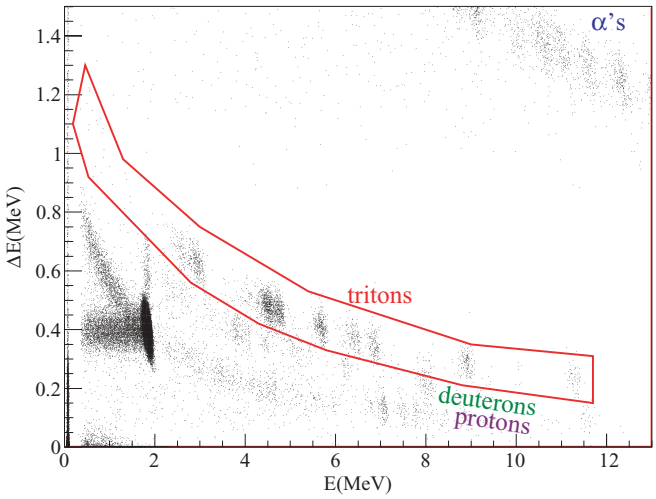

FIG. 2. (Color online) Particle identification spectra in ΔE-E silicon telescopes from ^{7}Li(^{14}C,t) run. The x and y axes are energies in MeV deposited by the charged particles in the E and ΔE detectors, respectively. The intense group of protons at 2 MeV (2.4 MeV total energy) corresponds to elastic scattering of ^{14}C by the hydrogen contamination in the ^{7}Li target. Tritons from the ^{7}Li(^{14}C,t) reaction are highlighted.

0° in the laboratory frame in inverse kinematics. Therefore, to measure the reaction cross section in the region of its maximum, the detectors were placed near 0° in the laboratory frame. The detector nearest to 0° was shielded from Rutherford scattering of the carbon beam on the lithium target with a 5-μm Havar foil in front of the telescope. This foil was thick enough to stop all of the carbon beam, but thin enough so that energy losses of the deuterons and tritons were small.

The ^{14}C beam energy is determined by the condition that the reaction c.m. energy should be below the Coulomb barrier in both the entrance and exit channels. The ^{14}C beam energies of 8.8 MeV for the ^{6}Li target (2.64 MeV in c.m.) and 11.5 MeV for the ^{7}Li target (3.83 MeV in c.m.) meet this requirement for the population of near-α-threshold states in ^{18}O.

III. ANALYSIS OF THE α-TRANSFER CROSS SECTIONS AND ANCS

Spectra of deuterons from the ^{6}Li(^{14}C,d) reaction and tritons from the ^{7}Li(^{14}C,t) reaction at 8.8 and 11.5 MeV of ^{14}C beam energy, respectively, are shown in Figs. 3 and 4. Peaks in the spectra correspond to the states or groups of states in ^{18}O, and all of them can be identified with the known states in ^{18}O. The near-threshold states of astrophysical interest for this work are the 1^- at 6.198 and the 3^- at 6.404 MeV. Peaks that correspond to these states appear at 2.5 and 3.0 MeV in Figs. 3 and 4, respectively. The experimental resolution of our setup in the c.m. was 120 keV (full width at half maximum); therefore these two states partially overlap. The following steps were performed to reduce the ambiguity in the extraction of cross sections from the measured spectra. The experimental resolution was accurately determined from the width of the peak corresponding to the 1^- state at 4.456 MeV. This state is separated from the other ^{18}O states by more than 500 keV

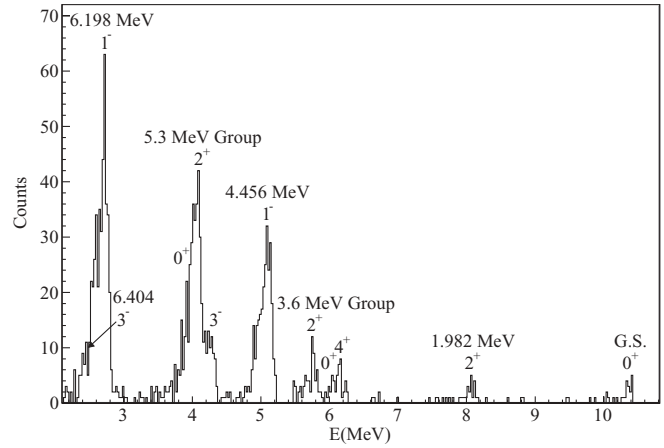

FIG. 3. Spectrum of deuterons from the ^{6}Li(^{14}C,d) reaction, measured by the 8° telescope at 8.8 MeV ^{14}C beam energy. The energy of the deuterons in the laboratory reference frame is shown on the x axis. The ^{18}O states populated in this reaction are labeled.

and is therefore well resolved in our spectra. It was observed that the shape of the 1^- peak is slightly asymmetric with a characteristic "tail" at the lower energy end (see the inset in Fig. 4) probably due to radiation damage in the detectors. This detector response was then used in the subsequent analysis by modeling it with a Gaussian function that has larger σ below the centroid energy and lower σ above the centroid energy (110 and 60 keV in the laboratory frame, respectively). All the peaks in the spectra are then fitted using this line shape.

Three states can contribute to the broad peak observed at ~3 MeV in the triton and ~2.5 MeV in the deuteron spectra. These are not only the aforementioned 1^- and 3^- at 6.198 and 6.404 MeV but also the 2^- at 6.35 MeV. While this last state is an unnatural parity state and cannot be populated in a direct α-transfer reaction, it can still contribute through the

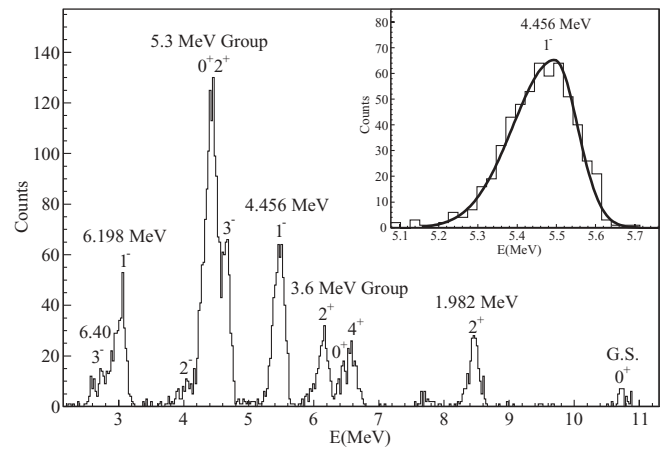

FIG. 4. Spectrum of tritons from the ^{7}Li(^{14}C,t) reaction, measured by the 8° telescope at 11.5 MeV ^{14}C beam energy. The energy of the tritons in the laboratory reference frame is shown on the x axis. The ^{18}O states populated in this reaction are labeled. The inset shows the double Gaussian fit of the well-resolved 1^- state at 4.456 MeV, which was used to determine the energy resolution of the experimental setup.

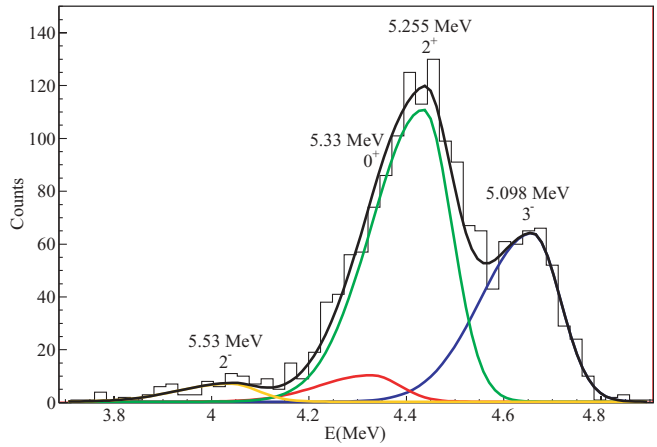

FIG. 5. (Color online) Four-state fit of the 4.5 MeV group of tritons from the ^{7}Li(^{14}C,t) reaction. This fit was performed to determine the strength of the unnatural parity 2^- state at 5.53 MeV, which was used to evaluate the contribution of the compound nucleus mechanism to the measured cross sections.

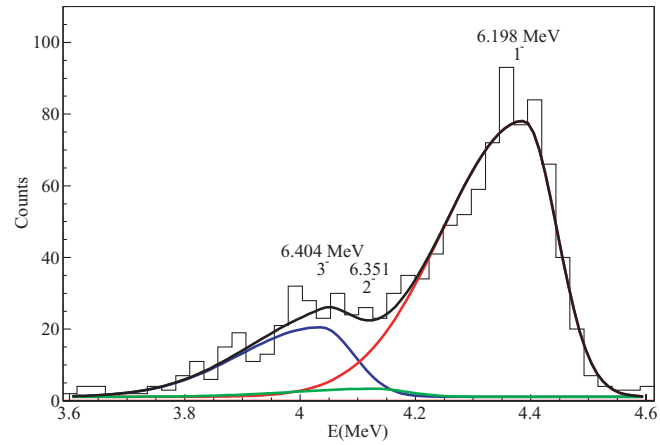

FIG. 6. (Color online) Fit of the triton spectrum from the ^{7}Li(^{14}C,t) reaction in the vicinity of 6.3 MeV of ^{18}O excitation energy. The black curve is the sum of the contributions from three states: the 1^- at 6.198, the 2^- at 6.35, and the 3^- at 6.404 MeV. The red, blue, and green lines represent individual contributions of the 1^-, 3^-, and 2^- states, respectively. The contribution of the 2^- state was not varied (see discussion in the text).

compound nucleus reaction mechanism. The magnitude of this contribution can be estimated using the 2^- state at 5.53 MeV as a benchmark. This state is clearly visible in the group of states at ∼4.5 MeV in the spectrum of tritons from the ^{7}Li(^{14}C,t) reaction (see Fig. 5). Four states contribute to this peak: the 2^- at 5.53, the 0^+ at 5.336, the 2^+ at 5.255, and the 3^- at 5.098 MeV. The four-state fit of the peak is shown in Fig. 5. There is also an unnatural parity 3^+ state at 5.378 MeV, but its contribution is expected to be very small, and since it has an excitation energy close to the 0^+ its possible contribution to the peak can be taken into account by overestimating the strength of the 0^+ state. Note that there are only four free parameters in this fit: the strengths of the four states. The positions of the states were fixed from the known values, and the width was determined by the experimental shape as modeled above. In this way, the cross section for population of the 2^- state at 5.53 MeV was determined. Assuming that only the compound nucleus mechanism is responsible for population of the unnatural parity 2^- state at 5.53 MeV, one can determine the cross section for population of the 2^- state at 6.35 MeV using the Hauser-Feshbach formalism and scaling it to the 2^- state at 5.53 MeV.

A sample of the three states fit to the peak that corresponds to ∼6.3 MeV excitation in ^{18}O is shown in Fig. 6. The strengths of the 1^- and the 3^- states at 6.198 and 6.404 MeV are the only two free parameters. The strength of the 2^- state was fixed as described above. The same fitting procedure was performed for all telescopes. The angular distributions for the 6.198 and 6.404 MeV states from the ^{6}Li(^{14}C,d) and ^{7}Li(^{14}C,t) reactions are shown in Fig. 7.

DWBA analysis of the angular distributions was performed using the code FRESCO (version FRES 2.4) [13]. The optical model potential parameters for the DWBA calculations were adopted from Refs. [14] and [15] for the ^{6}Li(^{14}C,d) and ^{7}Li(^{14}C,t) reactions, respectively. The shape of the form factor potentials is from Refs. [16,17]. These parameters are summarized in Table I. It is important to note that both the 1^- and the 3^- states were treated as bound in the DWBA analysis, even though the 3^- is actually unbound by 177 keV. This is a good approximation, since this state decays only by γ emission. The dependence of the final result on the choice of the binding energy will be discussed later in this section. The DWBA calculations were performed for beam energies at the center of the target: 11.42 MeV for the ^{7}Li target measurements and 8.7 MeV for the ^{6}Li target measurements. The ANCs for the 1^- and 3^- states were extracted from the experimental data and the DWBA analysis. .

Following the results of Ref. [18], the ANC is defined in the following way. The radial overlap function of the bound state c consisting of two particles $a + b[c = (ab)]$ can be approximated by a model wave function

$$I^{c}_{(ab)lj}(r) = \sqrt{S^{c}_{(ab)lj}}\,\psi^{c}_{nlj}(r), \tag{5}$$

where $\psi^{c}_{nlj}(r)$ is the bound-state wave function for the relative motion of a and b, and $S^{c}_{(ab)lj}$ is the spectroscopic factor of the

TABLE I. Optical model parameters used in analysis of the ^{14}C(^{7}Li,t) and ^{14}C(^{6}Li,d) reactions.

Channel	V[a] (MeV)	R (fm)	a (fm)	W[a] (MeV)	W_d[b] (MeV)	R' (fm)	a' (fm)	R_c (fm)	Ref.
^{14}C + ^{7}Li	33.1	4.17	0.85	0.0	7.8	4.51	0.72	4.17	[15]
^{18}O + t	130.0	3.43	0.72	8.0	0.0	4.19	0.80	3.43	[15]
^{14}C + ^{6}Li	250.0	3.26	0.65	0.0	7.5	3.26	0.65	4.82	[14]
^{18}O + d	92.92	2.73	0.814	0.0	2.5	3.65	0.709	3.4	[14]
^{14}C + α	v	3.53	0.6					3.53	[17]
$\alpha + d$	v	1.9	0.65					1.9	[16]
$\alpha + t$	v	2.05	0.7					2.05	[16]

[a]Form factor: Woods-Saxon; v = varied to reproduce separation energies.

[b]Form factor: Woods-Saxon derivative, values do not include a regular factor of 4: $W = 4W_d$.

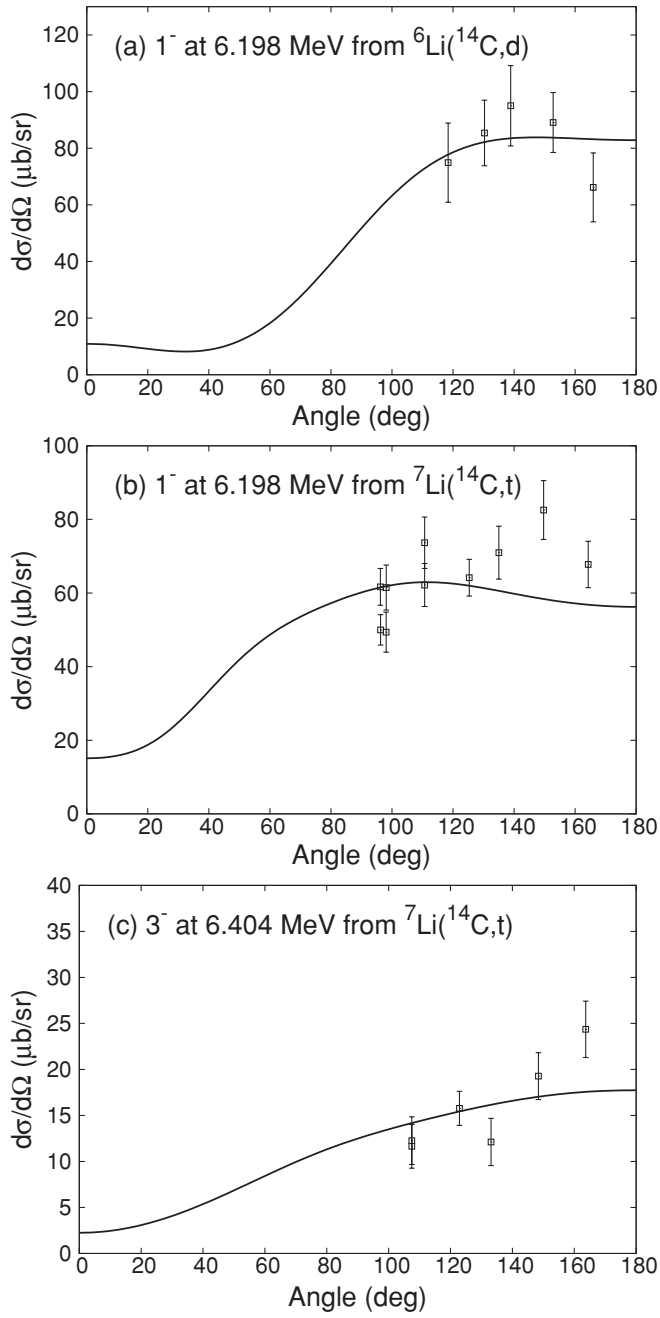

FIG. 7. Angular distributions for the 1^- at 6.198 and 3^- at 6.404 MeV states from the ^{6}Li(^{14}C,d) and ^{7}Li(^{14}C,t) reactions measured at 8.8 and 11.5 MeV, respectively. The solid lines correspond to the DWBA best fit.

configuration (ab) with the corresponding quantum numbers l and j in state c. The asymptotic normalization coefficient $C^c_{(ab)lj}$ defines the amplitude of the tail of the radial overlap function $I^c_{(ab)lj}$ and at radii beyond nuclear interaction radius ($r > R_N$) is given by

$$I^c_{(ab)lj}(r) \to C^c_{(ab)lj}\frac{W_{-\eta_c,l_c+1/2}(2k_{ab}r)}{r}. \quad (6)$$

$W_{-\eta_c,l_c+1/2}(2k_{ab}r)$ is the Whittaker function describing the asymptotic behavior of the bound-state wave function of two charged particles, k_{ab} is the wave number of the bound state c ($k_{ab} = \sqrt{2\,\mu_{ab}\varepsilon_c}$), and η_c is the Coulomb parameter $\eta_c = Z_a Z_b \mu_{ab}/k_{ab}$ of the bound state c. The bound-state wave function $\psi^c_{nlj}(r)$ has similar asymptotic behavior

$$\psi^c_{nlj}(r) \to b^c_{nlj}\frac{W_{-\eta_c,l_c+1/2}(2k_{ab}r)}{r}, \quad (7)$$

where b^c_{nlj} is the single-particle ANC. From Eqs. (5)–(7),

$$\left(C^c_{(ab)lj}\right)^2 = S^c_{(ab)lj}\left(b^c_{nlj}\right)^2. \quad (8)$$

Spectroscopic factors can be extracted directly from the experimental data

$$\frac{d\sigma}{d\Omega}_{\rm exp} = S_1 S_2 \frac{d\sigma}{d\Omega}_{\rm DWBA}, \quad (9)$$

where S_1 is the $\alpha + {}^{14}$C spectroscopic factor of the corresponding state in ^{18}O, and S_2 is the $\alpha + d(t)$ spectroscopic factor of the ground state of $^{6(7)}$Li. The squares of $\alpha + d(t)$ ANCs of the ground states of ^{6}Li and ^{7}Li are well known and equal to 5.29 ± 0.5 and 12.74 ± 1.1 fm^{-1}, respectively [19,20]. Therefore, the ANCs for the ^{18}O states populated in the (^{6,7}Li,d/t) reactions can be extracted. The R-matrix reduced width of the state can then be determined from the ANC [18] as

$$\gamma_c^2 = \frac{1}{2\,\mu_{ab}}\frac{W^2_{-\eta_c,l+1/2}(2k_{ab}R)}{R}\left(C^c_{(ab)lj}\right)^2, \quad (10)$$

where R is the channel radius. The partial α width Γ_α of the state, which is the only missing parameter needed to determine the astrophysically relevant resonance strength (see discussion in Sec. I), is given by Eqs. (2) and (3), in which γ_c^2 is used instead of $\gamma^2_{\rm SP}$.

The DWBA cross section is proportional to the squares of the single-particle ANCs determined by the form factor potentials. Spectroscopic factors are inversely proportional to the single-particle ANCs [see Eq. (8)]. This makes ANCs extracted from the experimental data using Eqs. (8) and (9) insensitive to the details of the form factor potentials. Since the reaction is performed at sub-Coulomb energies, the dependence of the DWBA cross section on the parameters of the optical model potentials is minimized.

The partial α width of the 3^- state at 6.404 MeV in ^{18}O determined from the measured cross sections using the approach described above is $\Gamma_\alpha = (7.8 \pm 2.7) \times 10^{-14}$ eV, and a detailed analysis of the parameter dependence of the result follows. The reduced width γ_α is inversely proportional, and the penetrability factor is directly proportional to the channel radius [see Eqs. (10) and (3)], so the explicit dependence of the partial α width on the channel radius cancels out. Only the implicit dependence through the kR argument of the Coulomb and Whittaker functions remains. The partial α width of the 3^- state calculated at the channel radius of 4 fm is 8.2×10^{-14} eV, and at the channel radius of 6 fm, it is 7.6×10^{-14} eV. Therefore, the channel radius uncertainty contributes to the total error budget at the level of 8%. A channel radius of 5.2 fm was adopted.

The value of the spectroscopic factor extracted from the transfer reaction depends on the assumption of the number of

radial nodes of the bound-state wave function, but the value of the corresponding ANC does not. The $\alpha + d(t)$ wave function that corresponds to the $^{6(7)}$Li ground state has one node (excluding the origin and infinity). The number of nodes of the $\alpha + {}^{14}$C wave function for the 3^- state in ^{18}O is not known. From the Talmi-Moshinski relation $2N + L = \sum(2n_i + l_i)$, where the sum is over all nucleons in the cluster, the minimum number of nodes in the α-cluster wave function of the 3^- state is two. The DWBA calculations for two-, three-, and four-node wave functions were performed producing $\Gamma_\alpha = (8.0, 7.9, \text{and } 7.8) \times 10^{-14}$ eV, respectively, so a 3% uncertainty is associated with the unknown number of nodes in the α-cluster wave function of the 3^- state at 6.404 MeV in ^{18}O. Three nodes were considered as the "best guess".

The 3^- state is unbound by 177 keV but treated as a bound state with small binding energy. The choice of binding energy is arbitrary and may, in principle, influence the final result. We performed calculations for several binding energies between 200 and 10 keV. While the dependence of the final result (value of Γ_α) on the specific value of the binding energy is very small, there is a clear trend of decreasing Γ_α with decreasing binding energy. Note that the penetrability factor was always calculated at resonance energy, which is 177 keV above the decay threshold. The extrapolation of this trend into the positive energy region suggests that the partial α width of a state at 177 keV in the c.m. should be reduced by about 2% from the value obtained with 30 keV binding. The final value of $\Gamma_\alpha = 7.8 \times 10^{-14}$ eV takes this small correction into account.

The ^{7}Li form factor potential was adopted from Ref. [16] (Woods-Saxon with $V = -91.2$ MeV, $R = 2.05$ fm, and $a = 0.7$ fm). This potential has been shown to reproduce $t + \alpha$ scattering phase shifts at low energies as well as the α-particle binding energy in ^{7}Li (with one node and an $\ell = 1$ wave function). It was used also as the main coupling potential for the $(^7\text{Li},t)\alpha$ transfer reaction. The dependence of Γ_α on the specific choice of the Li form factor shape parameters was investigated. An increase of the radius parameter from 2.05 to 3.7 fm (sum of the rms charge radius of the α particle and ^{3}H) increases Γ_α from 7.8×10^{-14} to 8.1×10^{-14} eV. The potential depth is always adjusted to reproduce the $\alpha + t$ binding energy with one node and an $\ell = 1$ wave function. Variation of the diffuseness parameter of this potential within reasonable limits (from 0.5 to 0.8 fm) has an even smaller influence on the final value of Γ_α ($\sim$2%).

The dependence of the final result on the specific parameters of the $^{14}\text{C} + \alpha$ binding potential is also weak. The ^{18}O form factor potential was taken from Ref. [17] (Woods-Saxon with $R = 3.53$ fm and $a = 0.6$ fm). The potential depth was adjusted to produce the desired binding energy. Variation of the radius parameter from 3.0 to 4.2 fm results in $\sim$4% variation of the partial α width, and variation of the diffuseness parameter from 0.5 to 0.8 fm produces $\sim$10% variation. Note that the DWBA cross section depends strongly on the specific choice of the form factor potential parameters and varies by an order of magnitude with the changes described above. However, the value of the ANC is not sensitive to these variations.

The influence of the optical model potential parameters on the final result was minimized by performing the α-transfer reaction at a sub-Coulomb energy. Yet, since the ^{14}C beam energy was close to the Coulomb barrier, the uncertainty in the parameters of the optical model potentials makes the largest contribution to the final uncertainty of the Γ_α value of the 3^- state. Assessment of this uncertainty is somewhat arbitrary but was determined here by performing a Monte Carlo variation of all the nuclear potential parameters. This process resulted in a Gaussian distribution of DWBA cross sections with a standard deviation of 30%. The radius and diffuseness changes to the imaginary part of the $^{14}\text{C} + {}^7$Li optical potential contributed the most to the uncertainty. DWBA calculations were performed with several different sets of $^{14}\text{C} + {}^7$Li potentials taken from Refs. [14,15,21] and verified that all of these (very different) potentials give Γ_α well within the 30% uncertainty limit determined using the Monte Carlo approach.

The statistical uncertainty for the $^7\text{Li}(^{14}\text{C},t)^{18}\text{O}(3^-)$ reaction data is 7%. The combined systematic uncertainty in the absolute cross section normalization originating from the determination of the product of the target thickness times the solid angle is also 7%. Finally, there is a 9% uncertainty in the known value of the $\alpha + t$ ANC, 12.74 ± 1.1 fm^{-1} [20]. Collecting all the components of the error budget yields a 35% final relative uncertainty in the Γ_α value of the 3^- state at 6.404 MeV in ^{18}O determined from the $^7\text{Li}(^{14}\text{C},t)\,\alpha$-transfer reaction at sub-Coulomb energy.

An ANC can only be reliably extracted from the transfer reaction data if the reaction is peripheral. Performing the transfer reaction at sub-Coulomb energy is an important factor in achieving this condition. Limiting the radius at which the transfer reaction is considered in DWBA calculations, it was verified that 95% of the transfer reaction cross section comes from a radius beyond 7 fm. This is far outside of the sum of nuclear interaction radii of ^{7}Li and ^{14}C, indicating that the reaction is highly peripheral.

The determination of the ANC of the 3^- state at 6.404 MeV in ^{18}O was also attempted from the $^6\text{Li}(^{14}\text{C},d)$ reaction data. Unfortunately, statistics were rather low, and only an upper limit could be set on the cross section from the $^6\text{Li}(^{14}\text{C},d)$ data. Therefore, only an upper limit of $\sim 10^{-13}$ eV can be determined for the Γ_α of this state, which is consistent with the $\Gamma_\alpha = (7.8 \pm 2.7) \times 10^{-14}$ eV determined from the $^7\text{Li}(^{14}\text{C},t)$ data.

The ANC for the 1^- state at 6.198 MeV and the corresponding uncertainty were determined using the same steps as outlined above. The only difference is that this state is bound by 29 keV with respect to α decay, therefore no correction to the dependence of the ANC on the assumed binding energy was necessary. The square of the Coulomb modified ANC for this state was extracted from both the $^7\text{Li}(^{14}\text{C},t)$ and the $^6\text{Li}(^{14}\text{C},d)$ data sets. The resulting values are 2.6 ± 0.9 and 3.0 ± 1.0 fm^{-1}. The two values extracted from the different reactions agree within error. As before, the uncertainty is dominated by the dependence on the optical model potential parameters. The final result for the squared Coulomb modified ANC of the 1^- state at 6.198 MeV in ^{18}O, determined by combining values from both the $(^6\text{Li},d)$ and $(^7\text{Li},t)$ measurements, is 2.8 ± 0.7 fm^{-1}.

IV. THE ^{14}C(α,γ) REACTION RATE

With the Γ_α for the 3^- state at 6.404 MeV and ANC for the 1^- at 6.198 MeV in ^{18}O, the ^{14}C(α,γ) reaction rate can be reliably extrapolated down to very low temperatures. At temperatures below 1 GK, four major contributors to the ^{14}C(α,γ) reaction rate can be identified. These are the direct capture (DC), the resonance capture through the 4^+ and 3^- states at 7.12 and 6.404 MeV, and the subthreshold resonance capture through the 1^- state at 6.198 MeV. Direct ^{14}C(α,γ) capture was measured by J. Görres *et al.* [9] in the energy range from 1.14 to 2.33 MeV and was extrapolated to lower energies using the following parametrization of the astrophysical S factor:

$$S(E) = 2.18 - 1.60E + 0.82E^2. \tag{11}$$

The resonance strength of the 4^+ state was also determined by direct measurements in Ref. [9] ($\omega\gamma = 0.46 \pm 0.08$ eV). The resonance strength of the 3^- state determined through the ANC in this work is $\omega\gamma = 7 \times \Gamma_\alpha = (5.5 \pm 1.9) \times 10^{-13}$ eV. The resonance reaction rate was calculated as in Ref. [22]

$$N_A\langle\sigma\nu\rangle_R = 1.54 \times 10^{11}(\mu T_9)^{-3/2} \times \omega\gamma \times \exp\left(\frac{-11.605E_r}{T_9}\right), \tag{12}$$

where μ is a reduced mass and T_9 is the temperature in GK.

The astrophysical S factor for the 1^- subthreshold resonance was calculated from the Coulomb modified ANC using the approach outlined in Ref. [18] as

$$S(E) \approx (2L+1)\pi^2 \frac{k_c}{\mu^2} \frac{\eta_c^{2L+1}}{(E+\varepsilon_c)^2} \Gamma_\gamma \times |\widetilde{C}_{1^-}|^2, \tag{13}$$

where $|\widetilde{C}_{1^-}|^2$ is the square of the Coulomb modified ANC [ANC divided by the corresponding Γ function, $\Gamma(L+1+\eta_c)$] of the 1^- state, k_c is the wave number of the 1^- state $k_c = \sqrt{2\mu\varepsilon_c}$, ε_c is the binding energy, and Γ_γ is the partial γ width of the 1^- state calculated from the known mean lifetime, $\Gamma_\gamma = (1.8 \pm 0.3) \times 10^{-7}$ MeV. The combined relative uncertainty of the $S(E)$ value is 30%. The S factor due to direct capture is compared with the S factor due to the 1^- subthreshold resonance in Fig. 8. It is important to note that at energies below 50 keV, the contribution to the S factor from the 1^- subthreshold resonance is larger than from the direct capture. Based on the results of Ref. [9], direct capture is mainly due to the p wave. Therefore, the direct-capture amplitude may interfere with the 1^- subthreshold resonance amplitude. The S factors due to constructive and destructive interference of these amplitudes are shown in Fig. 8 as red dotted and black dash-dotted curves, respectively. Obviously, interference significantly amplifies the importance of the 1^- state. Unfortunately, the sign of this interference is not known, and both cases will have to be considered. The reaction rates due to direct capture and capture to the subthreshold 1^- state at 6.198 MeV in ^{18}O were calculated by numerical integration of

$$\langle\sigma\nu\rangle_{NR} = \sqrt{\frac{8}{\mu\pi}}(kT)^{-3/2} \int S(E)\exp(-2\pi\eta) \times \exp\left(-\frac{E}{kT}\right) dE. \tag{14}$$

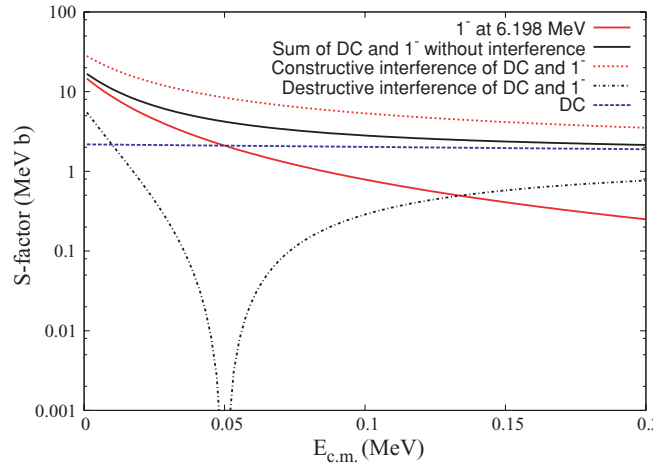

FIG. 8. (Color online) S factor of the ^{14}C(α,γ) reaction as a function of energy. The blue dashed line is the S factor due to direct capture (adopted from Ref. [9]), the red solid line is the S factor due to the subthreshold 1^- state at 6.198 MeV in ^{18}O, and the black solid line is the sum of the two without interference. The red dotted line corresponds to constructive and the black dash-dotted line to destructive interference of the 1^- state at 6.198 MeV with the direct-capture amplitude.

The reaction rates due to resonance and nonresonance capture are shown in Fig. 9 as a function of temperature. Three temperature regions can be identified. At $T > 0.3$ GK, the ^{14}C(α,γ) reaction rate is dominated by the 4^+ state at 7.12 MeV. The 4^+ resonance strength was measured directly [9,23], and the uncertainty of the ^{14}C(α,γ) reaction rate in this region is 17%. In the temperature range between 0.03 and 0.3 GK, the 3^- state at 6.404 MeV dominates. This temperature range is of particular interest for helium accreting white dwarfs and AGB stars. The 3^- resonance strength was determined in this work with an uncertainty of 35%, which

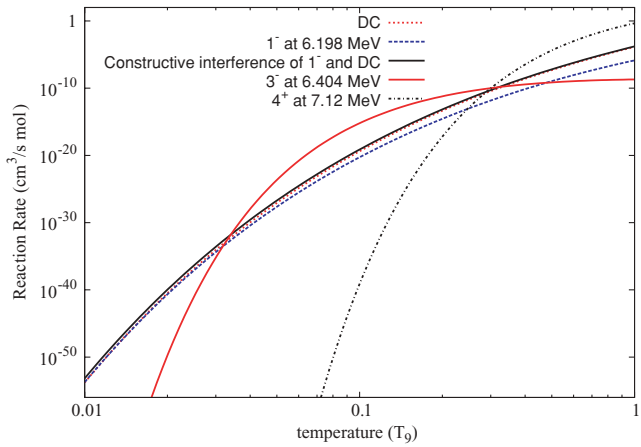

FIG. 9. (Color online) The ^{14}C(α,γ) reaction rate due to resonant and nonresonant capture. Resonant capture due to the 4^+ state at 7.12 and 3^- state at 6.404 MeV are shown as the black dash-dotted and solid red curves, respectively. Direct capture is the red dotted curve; capture due to the 1^- subthreshold resonance at 6.198 MeV is the blue dashed curve.

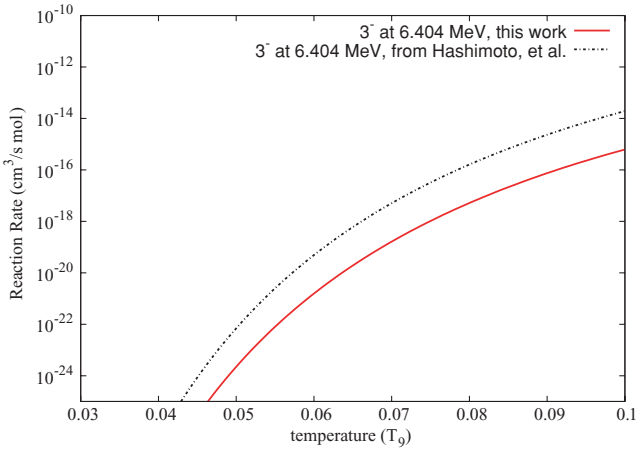

FIG. 10. (Color online) Comparison of the new $^{14}C(\alpha,\gamma)$ reaction rate (red solid curve) in the temperature range most relevant to the helium accreting white dwarfs and the rate used by Hashimoto *et al.* [6] (black dash-dotted curve).

determines the new uncertainty for the $^{14}C(\alpha,\gamma)$ reaction rate in the temperature range of 0.03–0.3 GK. Below 0.03 GK, direct capture and capture due to the subthreshold 1^- state at 6.198 MeV dominate. While direct capture was extrapolated from direct measurements in Ref. [9] and the S factor due to the 1^- subthreshold resonance was determined in this work with an uncertainty of 30%, the reaction rate at this low-energy region is still uncertain by two orders of magnitude because of the unknown interference between the direct and the 1^- subthreshold resonance capture amplitudes (see Fig. 8).

The new $^{14}C(\alpha,\gamma)$ reaction rate may have the most profound effect on the evolution of accreting helium white dwarfs. It was suggested by Hashimoto *et al.* [6] that under certain conditions the $^{14}N(e^-,\nu)^{14}C(\alpha,\gamma)^{18}O$ (NCO) reaction dominates over the 3α reaction and triggers a helium flash at earlier times and lower density values than the 3α process would otherwise. However, this suggestion is sensitive to the actual $^{14}C(\alpha,\gamma)$ reaction rate. Various accretion rates have been considered in Ref. [6], and it was concluded that the effect of the NCO reaction is larger for faster accretion. Following the evolutionary path of the central density and temperature of the helium accreting white dwarf with the accretion rate of $10^{-8} M_\odot \mathrm{yr}^{-1}$, it was found (see Fig. 5 in Ref. [6]) that ^{14}C burning is ignited when the central temperature reaches 0.066 GK, while the 3α reaction does not begin until 0.080 GK. This prediction was based on the hypothetical $^{14}C(\alpha,\gamma)$ reaction rate, which turned out to be a factor of 30 higher than the rate determined from our measurements. (Note that at these temperatures, the reaction rate is dominated by the resonance capture due to the 3^- state at 6.404 MeV). Comparison of the reaction rate in the temperature range of interest for helium accreting white dwarfs used by Hashimoto and the one determined from our experimental data is shown in Fig. 10. The new, much lower reaction rate would change the NCO ignition temperature to higher values. An estimate of the new ignition temperature based on equality of the corresponding $^{14}C(\alpha,\gamma)$ reaction rates gives a new value of about 0.075 GK, which is very close but still lower than the ignition temperature for the 3α reaction. Obviously, detailed calculations with the new $^{14}C(\alpha,\gamma)$ reaction rate are necessary to know whether the NCO reaction has an effect on the evolution of the helium accreting white dwarf. However, it is clear that the new, significantly reduced reaction rate casts serious doubt on the effectiveness of the NCO reaction chain as a trigger for helium flashes compared to the 3α reaction.

It was found in Ref. [8] that uncertainties in the $^{14}C(\alpha,\gamma)$ and the $^{19}F(\alpha,p)$ reaction rates are the main contributing factors to the uncertainty of the production of ^{19}F in AGB stars. The authors of Ref. [8] cite five orders of magnitude uncertainty in the $^{14}C(\alpha,\gamma)$ reaction rate due to the unknown spectroscopic factor of the 3^- state at 6.404 MeV. This uncertainty is eliminated now. Surprisingly, the "recommended" $^{14}C(\alpha,\gamma)$ reaction rate used in Ref. [8], which is based on the assumption that the spectroscopic factor of the 3^- state is 0.01, is almost exactly (within experimental uncertainty of this work) the same as the reaction rate determined from our measurements. This fortuitous coincidence means that the yields of ^{19}F calculated in Ref. [8] with the recommended $^{14}C(\alpha,\gamma)$ reaction rate are accurate, and no new calculations are necessary. Of course, the uncertainty due to the $^{19}F(\alpha,p)$ reaction rate still remains and will have to be addressed.

Finally, with the uncertainty for the $^{14}C(\alpha,\gamma)$ reaction rate reduced to just 35% in the temperature range of interest for the core helium flashes in low-mass stars, the debate over possible importance of the NCO reaction chain as a trigger can hopefully be settled.

V. CONCLUSION

The $^{14}C(\alpha,\gamma)$ reaction rate was studied using an indirect approach. The asymptotic normalization coefficients (ANCs) for the 1^- state at 6.198 MeV and 3^- at 6.404 MeV in ^{18}O were measured in the α-transfer reactions $(^7Li,t)$ and $(^6Li,d)$ on ^{14}C. The measurements were performed at sub-Coulomb energies to minimize the dependence of the final result on the optical model potential parameters. The extraction of ANCs instead of spectroscopic factors significantly reduced the dependence on the form factor potential parameters and the number of nodes assumed in the α-^{14}C wave function. The resonance strength of the 3^- state was determined from the ANC to be $\omega\gamma = (5.5 \pm 1.9) \times 10^{-13}$ eV. It was found that the resonance capture due to the 3^- state dominates the reaction rate in the temperature range of $0.03 < T_9 < 0.3$, which is the most relevant temperature range for the ^{19}F nucleosynthesis in AGB stars, evolution of helium accreting white dwarfs, and core helium flashes of low-mass stars. At temperatures below 0.03 GK, the $^{14}C(\alpha,\gamma)$ reaction rate is determined by the interplay between the direct capture and capture due to the subthreshold 1^- resonance at 6.198 MeV. The S factor due to the 1^- subthreshold state was determined in this work from the ANC, and the direct-capture S factor was suggested in Ref. [9]. In spite of this knowledge, the reaction rate at temperatures below 0.03 GK is still uncertain by two orders of magnitude thanks to the unknown interference (constructive or destructive) between the two amplitudes.

The new $^{14}C(\alpha,\gamma)$ reaction rate is a factor of 30 lower than the one used by Hashimoto *et al.* in Ref. [6]. Therefore, the importance of the NCO chain as a trigger for helium flashes in helium accreting white dwarfs suggested in Ref. [6] is reduced, if not eliminated all together. The recommended $^{14}C(\alpha,\gamma)$ reaction rate used in Ref. [8] for ^{19}F nucleosynthesis calculation in AGB stars fortuitously coincides with that determined from our experimental data, and the uncertainty of the ^{19}F production in AGB stars associated with the $^{14}C(\alpha,\gamma)$ reaction rate is now eliminated. We hope that the new information on the $^{14}C(\alpha,\gamma)$ reaction rate will help resolve the question of whether the NCO reaction chain can trigger helium flashes in cores of low-mass stars before the 3α reaction does.

ACKNOWLEDGMENTS

The authors are grateful to Peter Hoeflich and Akram Mukhamedzhanov for enlightening discussions and acknowledge support of the National Science Foundation under Grant No. PHY-456463.

[1] R. Mitalas, Astrophys. J. **187**, 155 (1974).
[2] K. Kaminisi, K. Arai, and K. Yoshinaga, Prog. Theor. Phys. **53**, 1855 (1975).
[3] R. G. Spulak, Astrophys. J. **235**, 565 (1980).
[4] K. Kaminisi and K. Arai, Phys. Rep. Kumamoto Univ. **6**, 13 (1983).
[5] K. Nomoto and D. Sugimoto, Publ. Astron. Soc. Jpn. **29**, 765 (1977).
[6] M. A. Hashimoto, K. Nomoto, K. Arai, and K. Kaminisi, Astrophys. J. **307**, 687 (1986).
[7] A. Jorissen, V. V. Smith, and D. L. Lambert, Astron. Astrophys. **261**, 164 (1992).
[8] M. Lugaro, C. Ugalde, A. I. Karakas, J. Görres, M. Wiescher, J. C. Lattanzio, and R. C. Cannon, Astrophys. J. **615**, 934 (2004).
[9] J. Görres, S. Graff, M. Wiescher, R. E. Azuma, C. A. Barnes, and T. R. Wang, Nucl. Phys. **A548**, 414 (1992).
[10] C. R. Brune, W. H. Geist, R. W. Kavanagh, and K. D. Veal, Phys. Rev. Lett. **83**, 4025 (1999).
[11] E. D. Johnson *et al.*, Phys. Rev. Lett. **97**, 192701 (2006).
[12] H. G. Bingham, A. R. Zander, K. W. Kemper, and N. R. Fletcher, Nucl. Phys. **A173**, 265 (1970).
[13] I. J. Thompson, Comput. Phys. Rep. **7**, 167 (1988).
[14] A. Cunsolo, A. Foti, G. Imme, G. Pappalardo, G. Raciti, and N. Saunier, Phys. Rev. C **24**, 476 (1981).
[15] H. T. Fortune and D. Kurath, Phys. Rev. C **18**, 236 (1978).
[16] K. I. Kubo and M. Hirata, Nucl. Phys. **A187**, 186 (1972).
[17] B. Buck, C. B. Dover, and J. P. Vary, Phys. Rev. C **11**, 1803 (1975).
[18] A. M. Mukhamedzhanov and R. E. Tribble, Phys. Rev. C **59**, 3418 (1999).
[19] L. D. Blokhintsev, V. I. Kukulin, A. A. Sakharuk, D. A. Savin, and E. V. Kuznetsova, Phys. Rev. C **48**, 2390 (1993).
[20] S. B. Igamov and R. Yarmukhamedov, Nucl. Phys. **A781**, 247 (2007).
[21] J. E. Poling, E. Norbeck, and R. R. Carlson, Phys. Rev. C **13**, 648 (1976).
[22] W. A. Fowler, G. R. Chaughlan, and B. A. Zimmerman, Annu. Rev. Astron. Astrophys. **13**, 69 (1975).
[23] M. Gai, R. Keddy, D. A. Bromley, J. W. Olness, and E. K. Warburton, Phys. Rev. C **36**, 1256 (1987).